

# Coherence and Instability in a Driven Bose-Einstein Condensate: A Fully Dynamical Number-Conserving Approach

T. P. Billam\* and S. A. Gardiner

Department of Physics, Durham University, Durham DH1 3LE, United Kingdom

(Dated: June 11, 2022)

We consider a Bose-Einstein condensate driven by periodic  $\delta$ -kicks. In contrast to first-order descriptions, which predict rapid, unbounded growth of the noncondensate in resonant parameter regimes, the consistent treatment of condensate depletion in our fully-time-dependent, second-order description acts to damp this growth, leading to oscillations in the (non)condensate population and the coherence of the system.

PACS numbers: 03.75.Kk 67.85.De 05.30.Jp

Central to the concept of a weakly interacting atomic Bose-Einstein condensate (BEC) is that each of the  $N$  component atoms can be considered to be in approximately the same motional state; this is manifest through the mean-field description of zero-temperature ( $T = 0$ ) BEC dynamics with the Gross-Pitaevskii equation (GPE), which takes the form of a single-particle Schrödinger wave equation with an additional cubic nonlinear term [1]. At finite temperature there is thermal depletion of the condensate, which can be theoretically accounted for in a variety of ways [2]. Even at  $T = 0$  in a system of finite size there is always a finite noncondensate fraction [1, 3], and one expects dynamics within the BEC to cause significant particle transfer from the condensate to the noncondensate fraction under quite general circumstances [4–7]. When rapid, such dynamical depletion has commonly been supposed to presage destruction of the BEC as a coherent entity, however previous studies have been hampered by the absence of a self-consistent treatment [6, 7]. Applying the number-conserving approach of Gardiner and Morgan [8], fully dynamically to second order, we have carried out the first such self-consistent treatment of a specific example system.

Our chosen test-system is based on the quantum  $\delta$ -kicked rotor [9–12], a paradigm quantum-chaotic system in which periodic driving leads to complex behavior, including dynamical localization [9, 12] and quantum resonances (associated with ballistic increase in the kinetic energy [9–11]). Atom-optical realizations of such systems [11–13] comprise an exciting area of research into quantum-chaotic phenomena; extension into the regime of BECs has also become an active area of research, in which several new phenomena have been predicted [6, 7, 14–16]. In the mean-field approximation, the GPE nonlinearity can strongly influence  $\delta$ -kicked-rotor-BEC dynamics [14]; in particular, the structure of quantum resonances was recently elucidated [16], revealing previously unobserved resonance profiles with a sharp asymmetric cut-off. The noncondensate fraction can be accounted for using a number-conserving approach [3, 4, 8, 17]: such approaches contain a fixed atom number (appropriate to atomic BEC experiments [8]), and nonlocal terms [ $\tilde{f}$  and  $Q$  in Eqs. (2) and (5)] which, within the second-order, linear-response treatment used by Morgan *et al.* [18], have proved vital in explaining the temperature dependence of collective excitation spectra

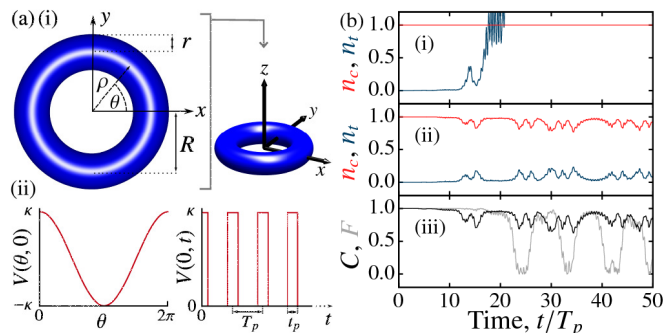


FIG. 1. (Color online) (a)  $\delta$ -kicked-rotor-BEC: (i) toroidally-trapped BEC; (ii)  $\delta$ -kicking potential. (b) Evolution of condensate and noncondensate fractions  $n_c = N_c/N$  and  $n_t = N_t/N$  in (i) first- and (ii) second-order number-conserving descriptions ( $N = 10^4$ ,  $g_T = 2.5 \times 10^{-4}$ ,  $T_p = 9.255$ ,  $\kappa = 0.5$ ). In (iii) we show the coherence measure  $C$  [Eq. (7)] in the second-order description, and the fidelity,  $F$  [Eq. (8)], of the condensate mode between descriptions.

observed at JILA and MIT [19]. The first-order, number-conserving description of Castin and Dum [4] [consisting of modified Bogoliubov-de Gennes equations (MBdGE) coupled to the GPE] has been the approach of choice in  $\delta$ -kicked BEC systems [6, 7]. This has revealed a general tendency towards rapid growth in the number of noncondensate atoms  $N_t$ . Such behavior is directly linked to linear dynamical instabilities (i.e., sensitivity to initial conditions in the linearized regime) in the GPE, enabled by its nonlinearity [5]; the presence of such instabilities is a generic feature of most nonlinear systems. Conversely, growth in  $N_t$  should match depletion in the condensate number  $N_c$ , and as atoms transfer from  $N_c$  to  $N_t$ , qualitatively one expects mean-field interactions and hence further transfer to “switch off” at some stage. Whether this occurs before the destruction of the condensate has remained an open question, as a linearized, first-order description treats the condensate as an effectively undepletable “particle bath,” feeling no effect from the noncondensate.

In this Letter we answer this question in the affirmative, using the first fully time-dependent application of the second-order, number-conserving description of Gardiner and Morgan [8], for a  $\delta$ -kicked-rotor-BEC in a quasi-one-dimensional ring trap [Fig. 1(a)], an ideal test system to explore generic in-

sues of dynamically induced condensate depletion. This self-consistent description consists of a *generalized GPE* (GGPE) coupled to the MBdGE; it explicitly preserves  $N = N_c + N_t$  and the orthogonality of the condensate and noncondensate, includes mutual interactions, and allows free transfer of population between the two. We solve these equations numerically and explore resonant parameter regimes which, to first order, lead to rapid, unbounded growth of the noncondensate. Our principal finding is the damping of this growth in the second-order description [Fig. 1(b)(i,ii)]. We also compute the coherence of the system and the departure of the second-order description from the GPE [Fig. 1(b)(iii)] for varying  $N$ . We show that, despite considerable differences in dynamics between the descriptions around resonant parameter regimes, the GPE accurately predicts the location of these parameter regimes; the cut-off identified in [16] is qualitatively preserved, however the accompanying exponential oscillations are strongly modified for experimentally realistic atom numbers.

We consider  $N$  bosonic atoms of mass  $M$ , held in a toroidal potential  $V_T(\rho, z) = M\omega^2[(\rho - R)^2 + z^2]/2$  [Fig. 1(a)(i)], interacting with  $s$ -wave contact interactions, and subject to a temporally and spatially periodic driving potential  $V(\theta, t)$  [Fig. 1(a)(ii)]; toroidal potentials similar to  $V_T$  can be created and precisely controlled using all-optical methods [20]. Assuming sufficiently strong radial and axial confinement, and harmonic length  $r \equiv \sqrt{\hbar/M\omega} \ll R$  [21], we reduce the system Hamiltonian to a dimensionless (length unit  $R$ , time unit  $MR^2/\hbar$ ), one-dimensional form [16]:

$$\hat{H} = \int d\theta \hat{\Psi}^\dagger(\theta) \left[ -\frac{1}{2} \frac{\partial^2}{\partial \theta^2} + V(\theta, t) + \frac{g_T}{2} \hat{\Psi}^\dagger(\theta) \hat{\Psi}(\theta) \right] \hat{\Psi}(\theta), \quad (1)$$

where the field operators obey bosonic commutation relations  $[\hat{\Psi}(\theta), \hat{\Psi}^\dagger(\theta')] = \delta(\theta - \theta')$ . The interaction strength  $g_T = 2a_s R/r^2$ , where  $a_s$  is the  $s$ -wave scattering length. As in [7, 16], we model the driving potential as a train of  $\delta$ -kicks,  $V(\theta, t) = \kappa \cos(\theta) \sum_{n=0}^{\infty} \delta(t - nT_p)$ , with (dimensionless) kicking period  $T_p$ . This may be approximated in experiment using short pulses of off-resonant laser light [10–12, 22].

We define the condensate mode  $\psi(\theta)$  (with creation operator  $\hat{a}_c^\dagger$ ) as the eigenfunction of the single-body density matrix  $\langle \hat{\Psi}^\dagger(\theta') \hat{\Psi}(\theta) \rangle$  with the largest eigenvalue  $N_c$  (the number of condensate atoms), to which it is normalized, i.e.,  $\int d\theta |\psi(\theta)|^2 = N_c \equiv \langle \hat{a}_c^\dagger \hat{a}_c \rangle$ . Hence, we expand the field operator as  $\hat{\Psi}(\theta) = \hat{a}_c \psi(\theta) / \sqrt{N_c} + \delta \hat{\Psi}(\theta)$ , where  $\delta \hat{\Psi}(\theta) \equiv \int d\theta' Q(\theta, \theta') \hat{\Psi}(\theta')$  describes the field component orthogonal to the condensate, and the projector  $Q(\theta, \theta') = \delta(\theta - \theta') - \psi(\theta) \psi^*(\theta') / N_c$ . We propagate  $\psi(\theta)$  with the GGPE:

$$i \frac{\partial \psi(\theta)}{\partial t} = \left\{ H_{\text{GP}}(\theta) - \lambda_2 + g_T \left[ 2\tilde{n}(\theta, \theta) - \frac{|\psi(\theta)|^2}{N_c} \right] \right\} \psi(\theta) + g_T \tilde{m}(\theta, \theta) \psi^*(\theta) - g_T \tilde{f}(\theta), \quad (2)$$

where  $\lambda_2$  is a real-valued scalar constant with a role similar to the chemical potential in grand-canonical treatments [23], and

$$H_{\text{GP}}(\theta) \equiv -\frac{1}{2} \frac{\partial^2}{\partial \theta^2} + V(\theta, t) + g_T |\psi(\theta)|^2. \quad (3)$$

Introducing the number-conserving fluctuation operator  $\tilde{\Lambda}(\theta) \equiv \hat{a}_c^\dagger \delta \hat{\Psi}(\theta) / \sqrt{N_c}$  [8], we define  $\tilde{n}(\theta, \theta') \equiv \langle \tilde{\Lambda}^\dagger(\theta') \tilde{\Lambda}(\theta) \rangle$  and  $\tilde{m}(\theta, \theta') \equiv \langle \tilde{\Lambda}(\theta') \tilde{\Lambda}(\theta) \rangle$  (the noncondensate normal and anomalous averages), and

$$\tilde{f}(\theta) \equiv \frac{1}{N_c} \int d\theta' |\psi(\theta')|^2 [\tilde{n}(\theta, \theta') \psi(\theta') + \psi^*(\theta') \tilde{m}(\theta', \theta)], \quad (4)$$

which ensures orthogonality of the condensate from the noncondensate component. The dynamics of  $\psi(\theta)$  are therefore coupled to those of  $\tilde{\Lambda}(\theta)$ ,  $\tilde{\Lambda}^\dagger(\theta)$ . We decompose  $\tilde{\Lambda}(\theta) = \sum_{k=1}^{\infty} [\tilde{b}_k u_k(\theta) + \tilde{b}_{-k} u_{-k}(\theta) + \tilde{b}_k^\dagger v_k^*(\theta) + \tilde{b}_{-k}^\dagger v_{-k}^*(\theta)]$ , where  $\tilde{b}_k, \tilde{b}_k^\dagger$  are bosonic quasiparticle operators, and the quasiparticle modes are normalized to  $\int d\theta [u_k(\theta)^2 - |v_k(\theta)|^2] = 1$ , and choose all time-dependence to be within the quasiparticle mode functions. These are then propagated by the MBdGE:

$$i \frac{\partial}{\partial t} \begin{pmatrix} u_k(\theta) \\ v_k(\theta) \end{pmatrix} = \int d\theta' \begin{pmatrix} L(\theta, \theta') & M(\theta, \theta') \\ -M^*(\theta, \theta') & -L^*(\theta, \theta') \end{pmatrix} \begin{pmatrix} u_k(\theta') \\ v_k(\theta') \end{pmatrix}, \quad (5)$$

where  $L(\theta, \theta') = \delta(\theta - \theta') [H_{\text{GP}}(\theta') - \lambda_0] + g_T \int d\theta'' Q(\theta, \theta'') |\psi(\theta'')|^2 Q(\theta'', \theta')$ ,  $M(\theta, \theta') = g_T \int d\theta'' Q(\theta, \theta'') \psi(\theta'')^2 Q^*(\theta'', \theta')$ , and  $\lambda_0$  [the system ground state value of  $(1/N_c) \int d\theta \psi^*(\theta) H_{\text{GP}}(\theta) \psi(\theta)$ ] is a lower-order approximant to  $\lambda_2$ . At  $T = 0$ , we can thus at all times express  $\tilde{n}(\theta, \theta') = \sum_{k=1}^{\infty} [v_k(\theta) v_k^*(\theta') + v_{-k}(\theta) v_{-k}^*(\theta')]$ ,  $\tilde{m}(\theta, \theta') = \sum_{k=1}^{\infty} [u_k(\theta) v_k^*(\theta') + u_{-k}(\theta) v_{-k}^*(\theta')]$ . The  $k$  index quantifies the momentum associated with the equilibrium quasiparticle eigenmodes, prior to application of  $V(\theta, t)$ . The coupling of Eq. (2) and Eq. (5) constitutes the second-order, number-conserving description of Gardiner and Morgan [8], and represents the equation of motion for  $\hat{\Psi}(\theta)$  expanded to second order in the fluctuation operator  $\tilde{\Lambda}(\theta)$  [24]. To first-order [4, 17] one obtains the GPE  $i\partial\psi(\theta)/\partial t = [H_{\text{GP}}(\theta) - \lambda_0]\psi(\theta)$ , coupled to the MBdGE [Eq. (5)], as used in previous time-dependent studies of noncondensate dynamics of  $\delta$ -kicked BECs [6, 7]. The GPE alone constitutes a zeroth-order description, although it may be possible to infer higher-order processes from a pure GPE treatment [16]; unlike GPE plus MBdGE, this is at least an internally consistent theoretical description [2, 8].

We take the  $T = 0$  equilibrium state (without driving) as our initial condition. The initial condensate mode is therefore spatially homogeneous:  $\psi = \sqrt{N_c/2\pi}$ . This sets  $\lambda_0 = g_T N_c/2\pi$ , and the initial stationary quasiparticle modes

$$\begin{pmatrix} u_k(\theta) \\ v_k(\theta) \end{pmatrix} = \frac{1}{2} \begin{pmatrix} A_k + A_k^{-1} \\ A_k - A_k^{-1} \end{pmatrix} \frac{e^{ik\theta}}{\sqrt{2\pi}}, \quad (6)$$

where  $A_k = A_{-k} = (1 + 4\lambda_0/k^2)^{-1/4}$ . Hence,  $N_t \equiv N - N_c = \int d\theta \tilde{n}(\theta, \theta) = (1/2) \sum_{k=1}^{\infty} (A_k - A_k^{-1})^2$ , and we set  $\lambda_2 = (g_T/2\pi)[N - 1 + \sum_{k=1}^{\infty} (A_k^2 - 1)]$ . To numerically determine a self-consistent  $T = 0$  solution to Eqs. (2) and (5), for given values of  $N$  and  $g_T$ , we set  $N_c = N$ , and then; (a) calculate  $A_k$  up to a cut-off momentum  $|k| = m$ ; (b) determine  $N_t$  from the  $A_k$ ; (c) make the replacement  $N_c = N - N_t$ . We repeat steps (a)–(c) until convergence. To determine the driven dynamics,

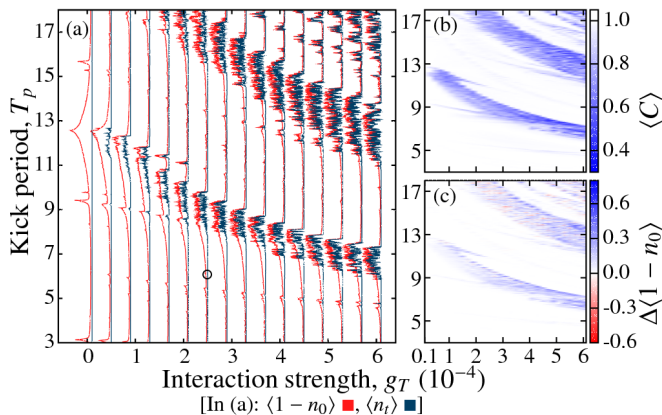


FIG. 2. (Color online) BEC response in the second-order description ( $N = 10^4$ ,  $\kappa = 0.5$ ): (a) relative population of  $k \neq 0$  momentum modes among all atoms,  $\langle 1 - n_0 \rangle$ , and noncondensate fraction,  $\langle n_i \rangle$ ; (b) coherence measure  $\langle C \rangle$  [Eq. (7)]; and (c)  $\langle 1 - n_0 \rangle$  as predicted by the GPE, minus its value in the second-order description. Averages are taken over the first 100 kicks.

we use a Fourier pseudospectral split-step method [25]; all simulations are converged in timestep, grid size, and quasi-particle cut-off momentum  $m$ .

In Fig. 1(b) we plot the condensate and noncondensate fractions ( $n_c = N_c/N$  and  $n_i = N_i/N$ ) for parameters which, in the first-order description, lead to rapid growth of the noncondensate (becoming unphysical after  $\sim 20$  kicks) [Fig. 1(b)(i)]. In the second-order description [Fig. 1(b)(ii)] the “back-action” of the noncondensate rapidly damps out this growth, leading instead to complementary oscillations in  $n_i$  and  $n_c$ . We also track the overall coherence of the system through

$$C = \iint d\theta d\theta' g_1(\theta, \theta') g_1(\theta', \theta), \quad (7)$$

where  $g_1(\theta, \theta') = \langle \hat{\Psi}^\dagger(\theta') \hat{\Psi}(\theta) \rangle / N$  is the first-order correlation function, and compare the evolution of  $\psi$  in the GGPE with the GPE prediction ( $\psi_{\text{GPE}}$ ) through the fidelity

$$F = \frac{|\int d\theta \psi_{\text{GPE}}^*(\theta) \psi(\theta)|^2}{NN_c}. \quad (8)$$

The quantity  $C$  equals unity only in the limit of a pure condensate, where the noncondensate fraction is exactly zero (i.e., the single-body density matrix is exactly factorizable). The GGPE then reduces to the GPE, and  $F = 1$ . Otherwise both  $C$  and  $F$  take values between zero and unity. In Fig. 1(b)(iii) we observe that  $C$  follows the oscillations of  $n_i$  closely, while  $F$  shows larger amplitude oscillations with revivals. Similar behavior persists across the  $T_p$ - $g_T$  parameter space: in Fig. 2(a) we show the time averaged response to weak driving ( $\kappa = 0.5$ ), by plotting  $1 - n_0$  averaged over the first 100 kicks; here  $n_k = \langle \hat{a}_k^\dagger \hat{a}_k \rangle / N$ , where  $\hat{a}_k^\dagger$  creates an atom with momentum  $k$ . The structure of this response over the range of Fig. 2(a), modeled with the GPE alone, was recently elucidated [16]: the response is dominated by linear resonances

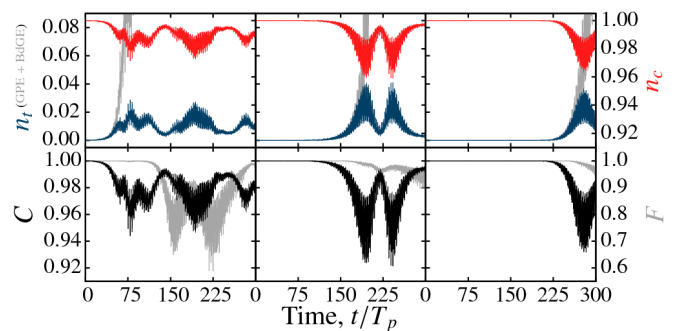


FIG. 3. (Color online) Comparison of first- and second-order descriptions close to a nonlinear resonance explored in [16] [ $g_T N = 2.5$ ,  $T_p = 6.12$ ,  $\kappa = 0.5$ : circle in Fig. 2(a)]. Condensate and noncondensate fractions  $n_c$  and  $n_i$ , coherence measure  $C$  [Eq. (7)], and the fidelity of the condensate mode between descriptions,  $F$  [Eq. (8)], are shown. Columns correspond (left to right) to  $N = 10^4$ ,  $10^8$ , and  $10^{12}$ ; agreement of the initial growth in  $n_i$  between the second-order (dependent on  $g_T$  and  $N$ ) and first-order (dependent on  $g_T N$ ) descriptions over such a range is a useful test of the second-order numerics.

corresponding to the first two primary quantum resonances of the  $\delta$ -kicked rotor as  $g_T \rightarrow 0$  [10]. Higher-order linear resonances generally decay with increasing  $g_T$ , while nonlinear resonances appear, with no analog in the linear regime [16]. To first-order (GPE plus MBdGE) all these resonant areas of parameter space are associated with rapid growth of the noncondensate fraction  $n_i$  due to linear instabilities in the GPE dynamics [7]. In contrast, we find that in the second-order description (GGPE plus MBdGE) this growth is damped out: throughout Fig. 2(a) the 100-kick average of  $n_i$  remains below 0.6. However,  $\langle n_i \rangle$  is still strongly enhanced in parameter regimes with significant resonant response [large  $\langle 1 - n_0 \rangle$ , as shown in Fig. 2(a)]. The predictions of the second-order description then differ considerably from the standalone GPE description, as shown by the behavior of  $\langle C \rangle$  [Fig. 2(b)], and the difference in response (as measured by  $\langle 1 - n_0 \rangle$ ) between descriptions [Fig. 2(c)]. Nonetheless, we find that the resonances are located in the same regions of parameter space in both descriptions, and that the asymmetric profiles and sharp cut-offs seen in [16] remain. Away from these resonances the GPE agrees well with the second-order description, up to the 100 kicks we consider.

In Figs. 3 and 4 we compare the first- and second-order descriptions, for varying  $N$  but fixed  $g_T N$ , close to a nonlinear resonance studied in [16] [circle in Fig. 2(a)]. Figure 3 shows that the dynamics in the second-order description match the GPE for times which increase with  $N$ . This increase is slow, however; for realistic  $N$  ( $\ll 10^8$ ) the loss of coherence, unaccounted for in the GPE and measured by decay in  $C$ , quickly becomes significant. Furthermore, in Fig. 4 we see that, on the same timescales associated with significant decay in  $C$ , the dynamics of the relative populations  $n_k$ , as studied in [16] using the GPE, noticeably differ in our second-order description. Compared to the first-order description, rapid growth of the noncondensate begins at the same time in our second-

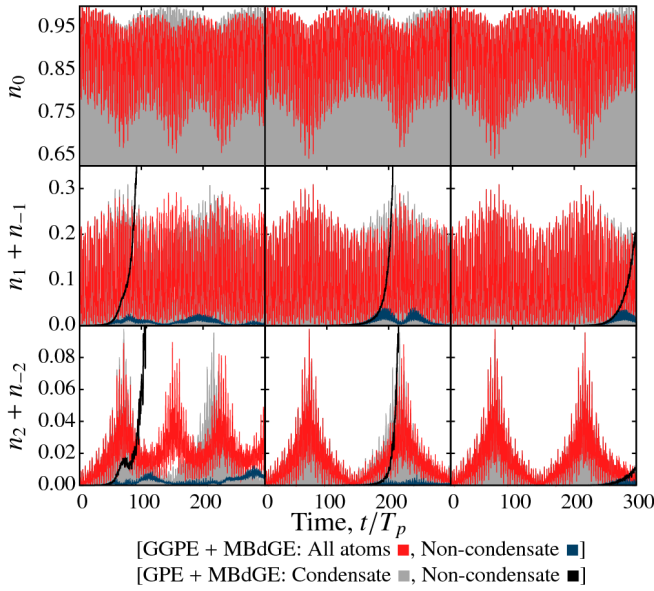


FIG. 4. (Color online) Relative populations,  $n_k$ , of low momentum modes in the first- and second-order descriptions (parameters as in Fig. 3). In the second-order description  $n_k$  is shown among all atoms and among the noncondensate atoms; in the first-order description  $n_k$  is shown among condensate atoms (as a bar chart) and among the noncondensate atoms (with a three-period moving average). Columns correspond (left to right) to  $N = 10^4$ ,  $10^8$ , and  $10^{12}$ .

order description. However, transfer of population to the non-condensate is driven by, and sensitive to, atom-atom interactions. Hence, decreasing population of the condensate, consistently accounted for in the second-order description, reduces the mean-field interactions, and hence the rate of population transfer. We observe population oscillations between condensate and noncondensate fractions, accompanied by oscillations in the coherence  $C$  and fidelity  $F$  [Fig. 3]. In Fig. 4 we also observe the exponential oscillations in  $n_2 + n_{-2}$  reported in [16]; however, for realistic atom numbers the frequency of these oscillations is quickly increased by the presence of a significant noncondensate fraction.

We have applied a fully dynamical, second-order, number-conserving approach [8] to the  $\delta$ -kicked-rotor-BEC. In contrast to a first-order approach, we observe that rapid growth of the noncondensate in resonant parameter regimes is damped by our consistent treatment of the condensate population and condensate-noncondensate interactions. Although our description leads to different dynamics around resonant parameter regimes, these regimes occur where the GPE predicts them. Furthermore, our description retains the cut-offs, but will typically strongly modify the exponential oscillations predicted by the GPE. Extension of our second-order description to other BEC systems offers exciting possibilities for future research.

We thank T. S. Monteiro and M. D. Lee for discussions, the UK EPSRC (Grant No. EP/G056781/1), the Jack Dodd Centre (S.A.G.) and Durham University (T.P.B.) for support.

\* t.p.billam@durham.ac.uk

- [1] L. Pitaevskii and S. Stringari, *Bose-Einstein Condensation* (Clarendon Press, Oxford, 2003).
- [2] P. B. Blakie *et al.*, *Adv. Phys.* **57**, 363 (2008); N. P. Proukakis and B. Jackson, *J. Phys. B* **41**, 203002 (2008).
- [3] Y. Castin and R. Dum, *Phys. Rev. A* **57**, 3008 (1998).
- [4] Y. Castin and R. Dum, *Phys. Rev. Lett.* **79**, 3553 (1997).
- [5] S. A. Gardiner, *J. Mod. Optics* **49**, 1971 (2002).
- [6] S. A. Gardiner *et al.*, *Phys. Rev. A* **62**, 023612 (2000); L. Rebuzzini *et al.*, *ibid.* **76**, 031603 (2007).
- [7] C. Zhang *et al.*, *Phys. Rev. Lett.* **92**, 054101 (2004); J. Liu *et al.*, *Phys. Rev. A* **73**, 013601 (2006); J. Reslen, C. E. Creffield, and T. S. Monteiro, *ibid.* **77**, 043621 (2008).
- [8] S. A. Gardiner and S. A. Morgan, *Phys. Rev. A* **75**, 043621 (2007).
- [9] G. Casati *et al.*, “Stochastic behavior in classical and quantum hamiltonian systems,” (Springer, Berlin, 1979) p. 334; F. M. Izrailev and D. L. Shepelyanskii, *Theor. Math. Phys.* **43**, 553 (1980).
- [10] M. Saunders *et al.*, *Phys. Rev. A* **76**, 043415 (2007).
- [11] C. Ryu *et al.*, *Phys. Rev. Lett.* **96**, 160403 (2006).
- [12] F. L. Moore *et al.*, *Phys. Rev. Lett.* **75**, 4598 (1995).
- [13] M. K. Oberthaler *et al.*, *Phys. Rev. Lett.* **83**, 4447 (1999); G. J. Duffy *et al.*, *Phys. Rev. A* **70**, 041602 (2004).
- [14] D. L. Shepelyansky, *Phys. Rev. Lett.* **70**, 1787 (1993); S. Wimberger *et al.*, *ibid.* **94**, 130404 (2005); L. Rebuzzini, S. Wimberger, and R. Artuso, *Phys. Rev. E* **71**, 036220 (2005).
- [15] B. Mieck and R. Graham, *J. Phys. A* **38**, L139 (2005).
- [16] T. S. Monteiro, A. Raçon, and J. Ruostekoski, *Phys. Rev. Lett.* **102**, 014102 (2009).
- [17] C. W. Gardiner, *Phys. Rev. A* **56**, 1414 (1997); M. D. Girardeau, *ibid.* **58**, 775 (1998); M. Girardeau and R. Arnowitt, *Phys. Rev.* **113**, 755 (1959).
- [18] S. A. Morgan *et al.*, *Phys. Rev. Lett.* **91**, 250403 (2003); S. A. Morgan, *Phys. Rev. A* **69**, 023609 (2004); **72**, 043609 (2005).
- [19] D. S. Jin *et al.*, *Phys. Rev. Lett.* **77**, 420 (1996); **78**, 764 (1997); M.-O. Mewes *et al.*, *ibid.* **77**, 988 (1996); D. M. Stamper-Kurn *et al.*, *ibid.* **81**, 500 (1998).
- [20] A. Ramanathan *et al.*, *Phys. Rev. Lett.* **106**, 130401 (2011); S. Franke-Arnold *et al.*, *Opt. Express* **15**, 8619 (2007).
- [21] P. L. Halkyard, M. P. A. Jones, and S. A. Gardiner, *Phys. Rev. A* **81**, 061602 (2010).
- [22] A qualitatively similar driving potential,  $V_2(\theta, t) = V(2\theta, t)$ , could be generated using counterpropagating Laguerre-Gaussian laser modes [L. Allen *et al.*, *Phys. Rev. A* **45**, 8185 (1992)], in which case  $\kappa = \Omega^2 t_p / 8\Delta$ , for laser detuning  $\Delta$ , Rabi frequency  $\Omega$ , and pulse duration  $t_p$ . Alternatively,  $V(\theta, t)$  could be generated by applying linear potential  $\kappa x / t_p R$  throughout the trap [15].
- [23]  $\lambda_2 = \text{Re}\{d\theta[H_{\text{GP}}(\theta)\psi(\theta) + \{g_T 2\tilde{n}(\theta, \theta) - |\psi(\theta)|^2/N_c\}\psi(\theta) + g_T \tilde{m}(\theta, \theta)\psi^*(\theta)]\psi^*(\theta)\}/N_c$ , evaluated for the ground state [8].
- [24] One must generally renormalize the ultraviolet divergence due to the anomalous average  $\tilde{m}$  in 3D; such infinities formally do not arise in 1D, however, making this procedure unnecessary.
- [25] This involves diagonalizing Eqs. (2) and (5) analytically for small timesteps, and reorthogonalizing  $\{u_k, v_k\}$  w.r.t.  $\psi$  after each timestep to prevent buildup of rounding errors.